Loss Models for Shaped Foil Windings on Low-Permeability Cores

J. D. Pollock
C. R. Sullivan

Found in *IEEE Power Electronics Specialists Conference,* June 2008, pp. 3122–3128.

Loss Models for Shaped Foil Windings on Low-Permeability Cores

Jennifer D. Pollock and Charles R. Sullivan
jennifer.pollock@dartmouth.edu charles.r.sullivan@dartmouth.edu http://power.thayer.dartmouth.edu
Thayer School of Engineering
8000 Cummings Hall, Dartmouth College, Hanover, NH 03755, USA

***Abstract*—The cross section of foil windings used in ungapped, low-permeability cores can be modified to reduce total winding loss. The optimal cross-section shape is determined to have a linear cut out and a loss model is developed to calculate the winding loss in foil windings with this cross-section. The loss model shows excellent accuracy when compared to the loss determined by finite-element analysis. The loss model has been used to implement an optimization that determines the lowest loss cross-section for a particular application.**

I. Introduction

FOIL windings are used in applications with large dc currents because of their low dc resistance. The current in power conversion circuits is usually composed of a dc current with some ac ripple at the switching frequency riding on it. Therefore, it is desirable to develop foil windings with low ac and dc resistance. Low-permeability cores are often used in inductors that handle large dc currents because most low-permeability materials perform well under dc bias. The inductance of these components rolls off slowly as the dc magnetizing force is increased, particularly when compared to the rolloff of components with gapped ferrite cores. This feature provides additional protection to the circuit against overload conditions which is desirable in several power conversion applications. Low-permeability cores without discrete air gaps are also used to avoid the windings losses that result from the air gap fringing field impinging on the winding. This paper presents a loss model for a new foil-winding configuration that reduces the ac resistance of foil windings on ungapped, low-permeability cores while maintaining a low dc resistance. This is accomplished by adjusting the shape of the winding cross section to optimize the tradeoff between ac and dc power loss.

The effect of the shape of the cross-section of a foil winding on the total winding loss has been investigated in [1], [2], [3]. The idea of shaping the foil to reduce losses is examined in [1] where the foil is curved to match the shape of the magnetic field in the winding window in high-permeability gapped cores. While this idea works to reduce the winding losses, the final design is difficult to manufacture and, therefore, it is not used in practice. In [2], the cross-section of a foil winding is "shaped" to match the magnetic field in a gapped, high-permeability core. Conductor is removed or cut away from the area where the fringing-field is the strongest (due to the air-gap), thus creating a notch in the winding cross-section. It is similar to the shape-optimized winding cross-sections proposed in [4], [5], [6] for solid wire or litz-wire windings in inductors with gapped, high-permeability cores. In [3], a model is developed and used to determine the optimal size of the cut-out by considering the tradeoff between dc and ac winding loss that gives the lowest total winding loss in inductors with gapped, high-permeability cores. The idea of shaping the cross-section of a foil winding is extended to windings for ungapped, low-permeability cores in [3], but neither a loss model nor a design method are presented.

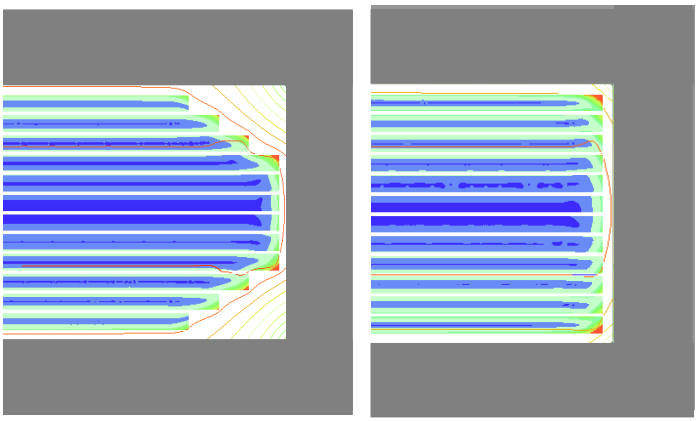

Fig. 1. FEA simulations showing the magnitude of the current density and the flux lines in a full-width foil winding on the right and a shaped foil winding on the left. The shaped cross section reduces the current density in the interior of the layers when compared to the full-width winding.

The contribution of this paper is to find the optimal winding shape for a winding with an ungapped, low-permeability core, develop a method to calculate the winding loss, and use the loss model to determine the winding dimensions that give the lowest total winding loss. The loss effects in foil windings with low-permeability cores are discussed in Section II. The optimal winding shape is determined in Section III. The power loss calculations used by the optimization are developed and verified for shaped foil windings in Section IV. The optimization method is described in Section V.

II. Winding Loss Effects in Distributed-Gap, Foil-Wound Inductors

It is difficult to accurately predict the winding loss in high-frequency foil windings using distributed-gap core configurations with analytical methods because the field in the winding window is not one-dimensional (1D). The distributed-gap core configuration considered here is created by using low-permeability core material without discrete air gaps in the magnetic path. At high

978-1-4244-1668-4/08/$25.00 ©2008 IEEE

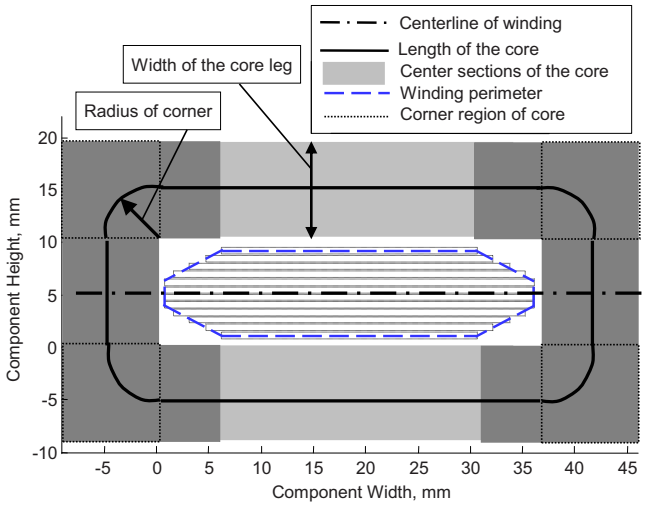

Fig. 2. The perimeter of the winding and the length of the core used in the loss model are defined. The end sections of the core are shaded with dark gray and the center sections of the core are shaded with light gray. The corner regions of the core are outlined with a dotted line.

frequencies, the current is going to flow in a distribution that minimizes the energy stored in the magnetic field. To do this, the high-frequency currents flow as close to the core as possible to minimize space between where the magnetomotive force (MMF) is created by the current in the winding and where it is dropped across the reluctance of the core.

Fig. 1 shows the current density and flux lines in a full-width foil winding on the right side and in a shaped foil winding on the left side. Both figures show the high-frequency current flowing on the surface of the winding, adjacent to the core. In both, the concentration of the high-frequency current in the corners of the winding is similar. However, the magnitude of the current density in the interior of the layers in the shaped foil winding is less than in the full-width foil winding and this contributes to a reduction in total winding loss. It is important to account for the winding loss that results from the current in the interior of each layer as well as the currents on surface of each layer to develop an accurate prediction of winding loss.

III. Determining the Optimal Winding Shape

We want to shape the winding cross section to provide the lowest total winding loss. To find the best type of shape, we determined the ac and dc resistances for a variety of different winding cross sections using finite-element analysis (FEA).[1] Fig. 3 shows the winding shapes investigated and the ac and dc resistance for each shape are shown in Fig. 4. Each point on the plot represents a different size cutout for a particular winding

[1]The proposed foil winding shapes were evaluated using a commercial finite-element package (Ansoft Maxwell) to understand the current distribution in the winding and to verify the accuracy of winding loss model presented here. FEA has been used to accurately predict the losses in magnetic components in published literature (e.g., [7]- [10]), so its validity will not be discussed here.

TABLE I
Parameters for Design Examples

Parameter	Design 1 Value and Units	Design 2 Value and Units	Design 3 Value and Units
Inductance	38 μH	152 μH	152 μH
Core	Magnetics Kool Mu DIN 55/25	same	$\frac{h_c}{b_c}$ = 0.5
Core μ	60	60	60
Number of turns	12	24	24
Foil thickness	0.70 mm	0.30 mm	0.524 mm
Insulation thickness	0.1 mm	0.1 mm	0.1 mm
I_{dc}	40 amps	20 amps	20 amps
$I_{ac,pp}$	16 amps	8 amps	8 amps
Frequency	50 kHz	50 kHz	50 kHz
Optimal cutout slope	0.26	0.28	0.48
Optimal cutout y-intercept	3.2 mm	3.2 mm	5.1 mm

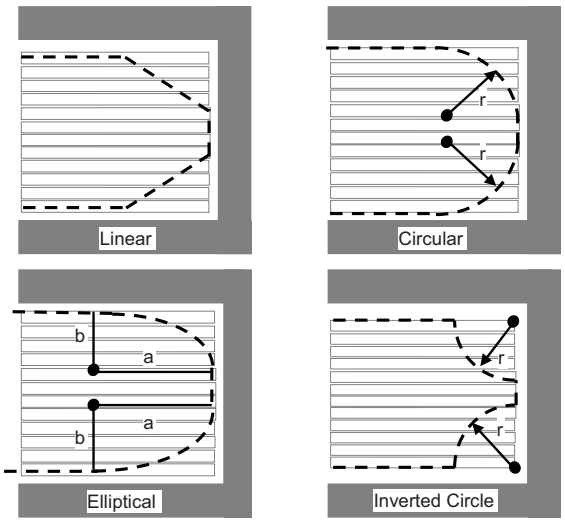

Fig. 3. A summary of the possible winding shapes investigated. Top left: linear. Top right: circular. Bottom left: elliptical. Bottom right: Inverted circle.

shape for design 1 described in Table I. A linearly shaped winding end showed the best performance, especially when a significant amount of conductor was cut away. In addition, the linear shape is the easiest to manufacture. Both a slope and a y-intercept are required to specify a linear shape, so several combinations were examined. The curve for the linear shape shown in Fig. 4 represents the slope and y-intercept combination that give the lowest ac resistance for a given dc resistance. Similarly, an ellipse is specified by two axes (a and b, defined in Fig. 3); Fig. 4 shows the results for several combinations of a and b.

IV. A Loss Model for Shaped-Foil Windings

The ac and dc power loss in the winding are calculated and summed to determine the total power loss. The dc resistance of a winding is found by $R_{dc} = \frac{\rho \ell_t N}{A_{foil}}$ where ρ is the resistivity of copper, ℓ_t is the average length of a turn, N is the number of turns, and A_{foil} is the cross-sectional area of the foil. The dc

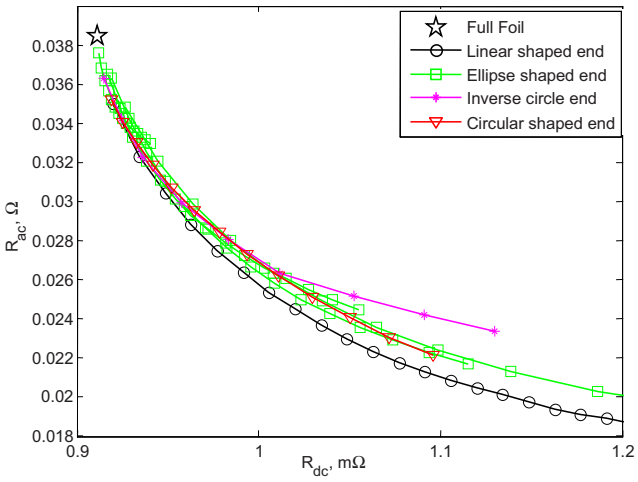

Fig. 4. The ac resistance is plotted verses the dc resistance for a variety of different shaped winding cross sections. The star shows the ac and dc resistance of the full-width foil winding for comparison. Refer to Fig. 3 to understand the legend descriptions.

power loss is calculated by $P_{dc} = R_{dc}I_{dc}^2$. The ac power loss is calculated by summing the loss at each harmonic of a triangular ripple current waveform. The net current in each layer is equal to the terminal current since the layers are connected in series. The terminal current in each layer is divided into a component that flows on the surface of the layer and a component that flows in the interior of the layer as described in Section IV-A. A method to calculate the power loss from the surface currents (surface power loss) is presented in Section IV-B. A method to calculate the power loss from the internal currents (internal power loss) is presented in Section IV-C.

A. Determining the Surface and Internal Currents

The total NI of the winding is assumed to flow on the surface of the winding, adjacent to the core. The surface of the winding is defined as the outer perimeter of the whole winding, not including the surfaces of individual layers that face other layers. The surface current includes the tip currents that flow on the ends or tips of each layer as well as the current on the outer surfaces of the top and bottom layers. A simple reluctance model of the core has been developed to split the total NI in the winding into a component for the center and end sections of the core (shown in Fig. 2). The ratio of the end reluctance (which include both ends of the core) to the total reluctance of the core is used to determine the amount of the total NI that flows on the ends of the winding. Because the permeability and cross-sectional area of the core are constant, the ratio of reluctance reduces to a ratio of length. The total length of the core is shown in Fig. 2. The length contributed by the corners of the core is approximated by a quarter of a circle with a radius equal to half the width of the core leg.

The ratio of the end reluctance to the total reluctance is

$$r_e = \frac{\ell_{core,end}}{\ell_{core,total}} \tag{1}$$

where $\ell_{core,end}$ is the length of the end sections of the core and $\ell_{core,total}$ is the total length of the core. The amount of the total current flowing on the ends of the winding is

$$I_{s,end} = r_e N I_t \tag{2}$$

where I_t is the terminal current.

The surface current flowing on the ends of the winding (equal to the sum of the tip currents) is assumed to be distributed uniformly around the perimeter of the shaped end for the purpose of calculating the winding loss due to these currents. However, the tip current in each layer must be determined because it is used to find the internal current in each layer. The current is distributed to the tips of each layer based on the ratio of the length along the winding end for a layer to the total length of the shaped winding ends.

The tip current in the i^{th} layer is

$$I_{tip,i} = \frac{\ell_{p,i}}{\sum_{i=1}^{N} \ell_{p,i}} I_{s,end} \tag{3}$$

where $\ell_{p,i}$ is the portion of the winding perimeter assigned to the i^{th} layer. The portion of the winding perimeter assigned to a specific layer is shown in Fig. 5. The length for a shaped layer is the distance from the center of that layer to the center of the layer below it, or the core wall if it is the bottom layer. The length for the first layer that is not cut (layer 5 in Fig. 5) is the layer height plus the length from the center of the layer below it to the bottom of the uncut layer. Any layer that is not cut has a length equal to a layer height, which is the sum of the foil thickness and insulation thickness.

With the tip currents in each layer determined, the internal currents, I_{int}, are given by

$$I_{int} = I_t - I_{tip}. \tag{4}$$

B. Surface Loss Model

The power loss due to the current flowing on the ends of the winding is determined by assuming the total end surface current, $I_{s,end}$, (found in (2)) flows uniformly in a layer one skin depth thick. The approximate power loss, $\tilde{P}_{s,end}$, is

$$\tilde{P}_{s,end} = I_{s,end}^2 \frac{\ell_{t,ave} N \rho}{\sum_{i=1}^{N} \ell_{p,i} \delta} \tag{5}$$

where δ is the skin depth. The loss given by (5) underestimates the surface loss compared to the loss determined by FEA, because (5) does not account for the large current densities in the corners of each layer. The loss calculated by (5) is scaled by a factor developed in [3] to account for current crowding in a similar situation with a circular cutout. Here, we modify the formula from [3] to apply to a linear cutout.

Excess loss, P_{excess}, is defined in [3] as:

$$P_{excess} = P_s - \tilde{P}_s \tag{6}$$

where P_s is the surface loss determined by FEA and $\tilde{P}_s$ is the approximate surface loss given by (5). The normalized excess loss factor, $\hat{P}_{excess}$, is the excess loss, P_{excess}, normalized to the

approximate surface loss, $\tilde{P}_s$. A dual-slope function [11] was used to fit a curve to the data:

$$\hat{P}_{excess}(X) = \frac{KX^{\alpha}}{(X^{-\beta n} + c^{-\beta n})^{\frac{1}{n}}} \tag{7}$$

where X is the ratio of the foil height to the skin depth. The constants K, α and β were chosen to fit (7) to the simulation data. The values of the curve fit constants are: n = 1.05, c = 1.366, K = 0.153, α = 0.06 and β = 1.93.

The surface loss factor (6) was developed for the situation in which the foil height and step size were equal. This is the case here only when the slope of the line defining the cutout is equal to one. In [3], the step size for each layer varies because the cutout is circular. To account for this, half of $\hat{P}_{excess}(X)$ was used in [3]. For the linear cutout proposed here, we multiply the normalized excess loss by $\sin(2\theta)$ where θ is the angle associated with the slope. The corrected estimate of the surface power loss is

$$\hat{P}_{s,end} = \tilde{P}_{s,end}(1 + \sin(2\theta)\hat{P}_{excess}(X)) \tag{8}$$

where $\hat{P}_{s,end}$ is the adjusted estimate of surface loss, $\tilde{P}_{s,end}$ is given by (5) and $\hat{P}_{excess}$ is given by (7).

C. Internal Power Loss Model

As shown in Fig. 1, the flux lines in the interior of the winding run parallel to the layers so the field can be considered 1D in this region. A 1D solution to Maxwell's equations was used to calculate the internal power loss as done in [3], using the following expression for loss per unit length from [12]

$$P_l = \frac{1}{2}\frac{b\rho}{\delta}\left[(H_a - H_b)^2 F(X) + 2H_a H_b G(X)\right] \tag{9}$$

where b is the width of foil, H_a is the magnetic field on one side of the conductor, and H_b is the magnetic field on the other side of the conductor. For the calculation of internal loss in each layer, the length of turn for that layer is used in order to account for the effects of turn length on loss. The functions $F(X)$ and $G(X)$ are

$$F(X) = \frac{\sinh(2X) + \sin(2X)}{\cosh(2X) - \cos(2X)} \tag{10}$$

$$G(X) = \frac{\sin(X) - \sinh(X)}{\cosh(X) + \cos(X)}. \tag{11}$$

Eq. (9) requires the magnitude of the field on each side of the conductor which is calculated from the internal currents found by (4). In an ungapped, low-permeability core configuration, the field is assumed to be maximum at the surface of the core and minimum in the center of the winding. To calculate the magnetic field on each surface of a layer, the field in the middle of the winding was assumed to be zero. Consider the winding shown in Fig. 5 with 12 layers. The field on the top of layer 6, $H_{a,N/2}$, is

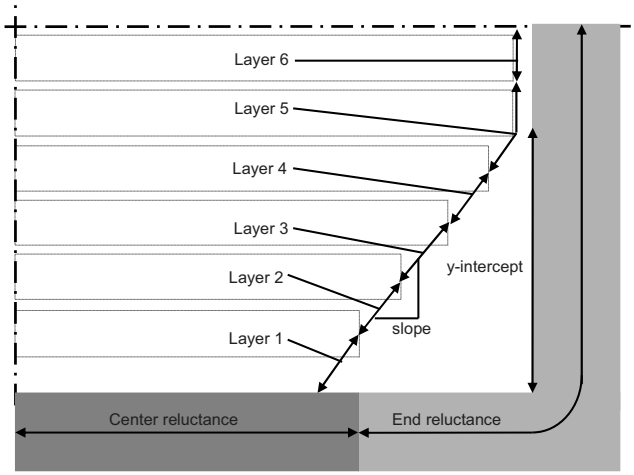

Fig. 5. The lower right hand corner of a shaped-foil winding is shown. The portion (length) of the winding perimeter assigned to each layer is shown. The slope and y-intercept defining the cutout are shown.

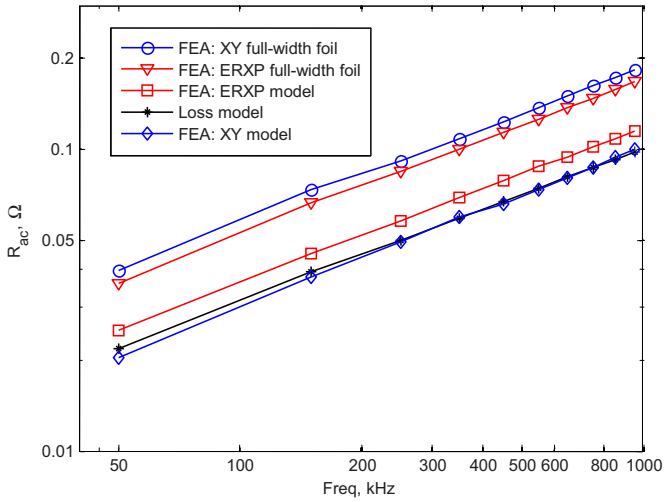

Fig. 6. The ac resistance predicted by the loss model for the shaped foil winding is compared to the ac resistance predicted by FEA. The ac resistance of the full-width foil winding is shown for comparison.

set to zero. By Ampere's law, the field at the opposite side of the same foil layer is

$$H_{b,N/2} = \frac{I_{int,N/2}}{b_{N/2}} \tag{12}$$

where $I_{int,N/2}$ is the internal current in the center layer, and $b_{N/2}$ is the width of the foil. To calculate the field at the surfaces of the following layers, $H_{a,i+1} = H_{b,i}$ is used, and the same approach is used to find the field between subsequent layers

$$H_{a,k} = \frac{\sum_{i=1}^{k} I_{int,i}}{b_k}. \tag{13}$$

The field on each side of the conductor is used in (9) to calculate the loss in each layer due to an internal current.

TABLE II
CURVE FIT CONSTANTS

Constant	Value
a_m	-5.6250
a_y	-17.2500
c_y	0.68
k_y	-1

D. Verification of Loss Calculation

The loss model presented here predicts the total loss for design 1 in Table I to be 5.74 W, which is 4% more than the loss determined by the two-dimensional (2D) FEA model in the XY plane of 5.50 W. The loss model was developed by considering a 2D model of the winding window (shown is Fig. 2) and accurately predicts the winding loss in a shaped foil winding according to the 2D FEA model. However, we are interested in windings for E cores which have more complex three-dimensional (3D) geometries in which there may be loss effects that are not captured by a single simple 2D FEA model. In order to evaluate some of the 3D effects, an equal-reluctance, extended-path (ERXP) FEA model [13] of the core was developed. An ERXP FEA model considers both the winding window cross section shown in Fig. 2 and the cross section perpendicular to that and combines them with a weighted average as described in [13].

The full-width foil winding was modeled using both these methods; the ac resistance predicted by each model is shown in Fig. 6. The ERXP model, which is shown to be more accurate in [13], predicts a smaller ac resistance for the full-width winding when compared to the 2D model. The shaped foil winding was also modeled using both the 2D and ERXP model. At 50 kHz, the ac resistance determined by the loss model is 21.8 mΩ, by the 2D FEA model is 20.4 mΩ and by the ERXP FEA model is 25.1 mΩ. The loss model under predicts the ac resistance by 6.6% when compared to the 2D FEA results, or by 13.2% when compared to the ERXP FEA results. According the ERXP model, the ac resistance of the full-width foil is 36.0 mΩ which is 43% higher than the ac resistance of the shaped-foil winding at 50 kHz.

V. OPTIMIZATION

An optimization program to design shaped-foil windings was developed in MATLAB [14]. The optimization determines the winding cross section with a linear cutout that minimizes the total power loss for a winding on an ungapped low-permeability core. We specify a linear cutout by the slope and intercept of the boundary line, as shown in Fig. 5. Based on the simulation results shown in Fig. 4, we have data on the best combinations of slope and intercept that give the lowest ac resistance for any given dc resistance. This data is plotted in Fig. 7 as a function of the dc resistance of a particular shaped winding, $R_{dc,s}$, normalized to the dc resistance of the full-width foil winding, $R_{dc,f}$. In addition, the y-intercept shown in Fig. 7 has been normalized to half the winding height

$$y_{norm} = \frac{y}{\frac{h_{winding}}{2}} \tag{14}$$

where y is the distance from a bottom of the winding and $h_{winding}$ is the height of the winding. We chose to normalize the dc resistance and y-intercept in an effort to extend the range of this optimization method to include other core geometries and foil-height to skin-depth ratios.

Exponential functions were fit to the data resulting in the relationship:

$$m\left(\frac{R_{dc,f}}{R_{dc,s}}\right) = m_{min} + (1 - m_{min})e^{(a_m \frac{R_{dc,s}}{R_{dc,f}})} \tag{15}$$

for the slope, m, as a function of the resistance ratio, where m_{min} is the minimum slope defined by the winding window height and width and

$$y_{norm}\left(\frac{R_{dc,f}}{R_{dc,s}}\right) = c_y + k_y e^{(a_y \frac{R_{dc,s}}{R_{dc,f}})} \tag{16}$$

for the normalized y-intercept. c, k, and a are constants found by curve-fitting. The values of these constants are listed in Table II. These two equations were combined so the optimal normalized y-intercept could be determined for a given slope:

$$y_{norm}(m) = c_y + k_y \left(\frac{m - m_{min}}{1 - m_{min}}\right)^{\frac{a_y}{a_m}}. \tag{17}$$

The ability to find the y-intercept for a given slope was developed in order to perform the optimization on a single variable, in this case, the slope. Given the method to calculate the power loss in Section IV, standard numerical optimization algorithms can be used to find the value of the slope that minimizes the total loss. The corresponding normalized y-intercept is found from (17). The slope and y-intercept of the optimal shape for design 1 are given in Table I. The verification of the loss calculation presented in Section IV-D was done for the foil winding shape determined by the optimization for design 1.

The optimization presented above was developed with design 1 and then applied to design 2 and 3 in Table I, in order to check that it works for other situations. Design 2 is the same as design 1 except the number of turns has been doubled from 12 to 24 and the ac and dc current have been cut in half. For design 2, the optimization determined that the lowest-loss shaped winding would have a slope of 0.35 and a y-intercept of 3.23 mm. An extensive search of over 200 winding cross-sections simulated with FEA, each with a different combination of slope and y-intercept, was performed to check that the optimization method was correctly identifying the lowest-loss shaped winding for design 2. From these simulations, the lowest-loss cross section had a slope of 0.35 and a y-intercept of 3.1 mm.

To compare the loss for the two similar cross sections, found with the optimization method and with an exhaustive FEA search, FEA was used. For the design chosen by the optimization method, the total loss was 4.62 W, and for the design chosen by the FEA simulation search, the total loss was 4.56 W. The total losses determined for the two winding cross sections were very close although the FEA simulations found a slightly lower loss cross section. This result shows that the optimization method developed here works to find the lowest-loss winding cross section. Furthermore, this demonstrates that the optimization can

TABLE III
SUMMARY OF RESULTS FOR DESIGN EXAMPLES

Parameter	Design 1		Design 2		Design 3	
Full foil total loss from FEA	8.35 W		10.71 W		10.76 W	
	Optimization	2D FEA search	Optimization	2D FEA search	Optimization	2D FEA search
Slope	0.26	0.35	0.28	0.35	0.48	0.55
Y-intercept	3.23 mm	3.20 mm	3.23 mm	3.10 mm	5.06 mm	6.2 mm
Total loss from FEA	5.74 W	5.50 W	4.62 W	4.56 W	6.05 W	5.62 W

find the lowest-loss winding cross-section for a different ratio of foil height to skin depth and a different number of turns; the optimization worked for design 2 even though it was developed using design 1.

The ratio of the winding window height to the winding window width is 0.28 for design 1 and 2. For design 3, this ratio was increased to 0.5 in order to examine the performance of the optimization on other core geometries. The optimization method developed here found that the lowest loss cross section would have a slope of 0.48 and a y-intercept of 5.1 mm. Another extensive round of FEA simulations was carried out on this design to check that the optimization method was correctly identifying the lowest-loss winding cross section. The FEA search found the lowest-loss cross section to have a slope of 0.55 and a y-intercept of the 6.1 mm. FEA was used to find the total loss for each cross section and determined the loss for the cross section found by the optimization method to be 6.05 W and the loss for the cross section found from the FEA simulation search to be 5.62 W. The total loss for the cross section found by the optimization is 7% higher than the total loss for the cross section determined by FEA. Even though the optimization did not find the absolute lowest-loss cross section, the optimization was still able to reduce the total loss by 45% compared to the full-width foil winding. This example demonstrates that the optimization can find winding cross sections that provide a substantial reduction in total loss relative to the traditional, full-width foil windings.

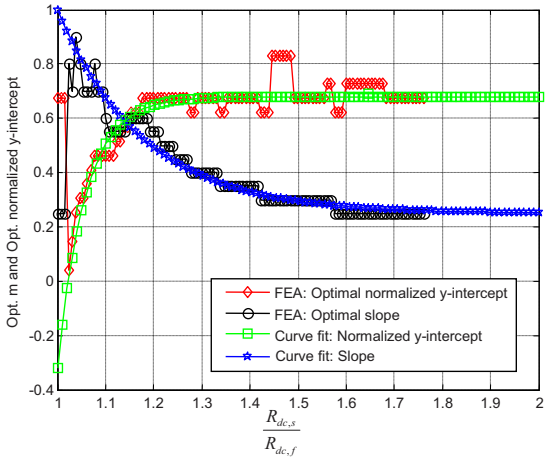

Fig. 7. The data collected for the optimal linear cutout winding for example design 1. A curve is fit for both the slope and normalized y-intercept. The relationship between the slope and normalized y-intercept used by the optimization is also shown.

VI. RESULTS AND CONCLUSIONS

Shaped-foil windings for ungapped, low-permeability cores offer a reduction in component loss and weight when compared to full-width foil windings. The results for all designs are summarized in Table III. For design 1, the total winding loss (including both dc and ac loss) was reduced by 18.5% from 7.74 W to 6.31 W (according to the ERXP FEA model) through the use of a shape-optimized foil winding. At 50 kHz, the ac resistance was reduced by 43%, from 36 mΩ for the full-width foil winding to 25 mΩ for the shape-optimized winding. As the magnitude of the peak-to-peak ac current increases relative to the dc current, the improvement available through the use a shaped foil winding increases. The loss model presented here accurately predicts the loss for design 1 with a shape-optimized foil winding to be 5.74 W compared to 5.50 W determined by FEA. The dc loss predicted by the model for the shaped winding (P_{dc} = 1.975 W) accounts for 34.4% of the total loss and the ac loss accounts for 65.6% of the total loss.

We have shown that the optimization method works for a different number of turns, a different foil-height to skin-depth ratio and a core geometry. The winding cross section found by the optimization for design 2 had 1.3% higher loss than the lowest-loss cross section found through an extensive FEA search. This example demonstrated the effectiveness of the optimization on windings with different foil height to skin depth ratios and different number of turns. The winding cross section found by the optimization for design 3 had 7% higher loss than the lowest-loss cross section found by the FEA search, but the shaped winding still reduced the total loss by 45% when compared to the full-width foil winding.

In addition to reducing the total winding loss, shaped-foil windings also reduce the weight of the winding. For design 1 in Table I, the winding weight was reduced by 56 g from 314 g to 258 g, or by 17.8%. Similar weight reductions were found for design 2 (16.8%) and design 3 (19.8%). This reduction is valuable in weight-sensitive applications and because of the high cost of copper. The combination of the loss reduction and weight reduction make these windings superior to traditional full-width foil windings.

REFERENCES

[1] A.J. Sinclair and J.A. Ferreira, "Optimal shape for ac foil conductors", in *Proceedings of PESC 1995 - Power Electronics Specialists Conference*, 1995, vol. 2, pp. 1064 – 1069.

[2] Jennifer D. Pollock and Charles R. Sullivan, "Gapped-inductor foil windings with low ac and dc resistance", in *39th Annual IEEE Industrial Application Society Conference*, 2004.

[3] Jennifer D. Pollock and Charles R. Sullivan, "Modelling foil winding configurations with low ac and dc resistance", in *36th Annual IEEE Power Electronics Specialists Conference*, 2005, pp. 1507–1512.

[4] Jiankun Hu and C. R. Sullivan, "Optimization of shapes for round-wire high-frequency gapped-inductor windings", in *Proceedings of the 1998 IEEE Industry Applications Society Annual Meeting*, 1998, pp. 900–906.

[5] Jiankun Hu and C. R. Sullivan, "Analytical method for generalization of numerically optimized inductor winding shapes", in *30th Annual IEEE Power Electronics Specialists Conference*, 1999, vol. 1, pp. 568–73.

[6] C.R. Sullivan, J.D. McCurdy, and R.A. Jensen, "Analysis of minimum cost in shape-optimized litz-wire inductor windings", in *IEEE 32nd Annual Power Electronics Specialists Conference*, 2001, pp. 1473–8 vol. 3.

[7] Liming Ye, G. R. Skutt., and R. Wolf F. C. Lee, "Improved winding design for planar inductors", in *PESC97. 28th Annual IEEE Power Electronics Specialists Conference*, 1997, pp. 1561–7 vol.2.

[8] G. R. Skutt and P. S. Venkatraman, "Analysis and measurement of high-frequency effects in high-current transformers", in *APEC '90. Fifth Annual Applied Power Electronics Conference and Exposition*, 1990, pp. 354–64.

[9] P. Alou, J. A. Cobos, R. Prieto, J. Uceda, and M. Roascon, "Influence of windings coupling in low-voltage dc/dc converters with single winding self-driven synchronous rectification", in *Proceedings of APEC 2000 - Applied Power Electronics Conference*, 2000, pp. 1000–5 vol.2.

[10] R. Prieto, J. A. Cobos, O. Garcia, P. Alou, and J. Uceda, "Model of integrated magnetics by means of "double 2d" finite element analysis techniques", in *30th Annual IEEE Power Electronics Specialists Conference*, 1999, pp. 598–603 vol.1.

[11] Xi Nan and Charles R. Sullivan, "An improved calculation of proximity-effect loss in high frequency windings of round conductors", 2003, vol. 2, pp. 853–860.

[12] J. H. Spreen, "Electrical terminal representation of conductor loss in transformers", *IEEE Transactions on Power Electronics*, vol. 5, no. 4, pp. 424–9, 1990.

[13] A.F. Hoke and C.R. Sullivan, "An improved two-dimensional numerical modeling method for e-core transformers", in *IEEE Applied Power Electronics Conference*, 2002, pp. 151–7 vol.1.

[14] The MathWorks, Inc., http://www.mathworks.com, *MATLAB Version 6*, 2000.